2008 IEEE Intelligent Vehicles Symposium
Eindhoven University of Technology
Eindhoven, The Netherlands, June 4-6, 2008

# An algorithm for Italian de-restriction signs detection

Claudio Caraffi, Elena Cardarelli, Paolo Medici, Pier Paolo Porta
VisLab – Dipartimento di Ingegneria dell'Informazione
Università degli Studi di Parma, ITALY
*http://vislab.it*
{caraffi,cardar,medici,portap}@vislab.it

Guido Ghisio and Gianluca Monchiero
Magneti Marelli Electronics Systems
Strategic Innovation & IP Mgt.
Venaria Reale (Torino), ITALY
guido.ghisio@mmarelli-se.com
gianluca.monchiero@mmarelli-se.com

***Abstract*— Color has proved to be an important feature to be exploited for road signs detection on images; however, not all road signs have distinctive color characteristics. This paper presents a shape-based approach for Italian de-restriction signs detection; the developed algorithm uses a black band extractor to highlight regions of interest, where a circle shape detection is performed. Tracking is used in order to increase reliability. The obtained detector is robust to different illumination conditions and shadows, and can manage different kinds of noise and perturbation. Despite its sensitiveness, the detector showed few false positives during performed tests.**

## I. INTRODUCTION

Providing systems for automatic signs detection is an important task to support drivers and improve safety on the road: in fact, by means of its visual code a road sign provides information that the driver should never miss, about either road conditions, dangers or proper behavior to be observed.

Road signs are usually painted with distinctive colors and many authors have used color-based detectors [2]–[5]; in [1] we presented a vertical traffic sign recognition system based on a three-step algorithm that uses color segmentation, shape recognition, and neural network to detect and classify almost all Italian traffic signs. The color-based approach faces difficulties when trying to detect European de-restriction signs ( [2], [3]) and in particular Italian ones (figure 1): the white color of this kind of signs is not a distinctive feature because it is not different from that of many elements in the image (e.g. the asphalt of the road) so that a color-based approach is not suitable to detect region of interest. On the other hand, in the development of a system capable to communicate current restrictions in any moment, discarding a de-restriction sign corresponds to give a false positive: in fact, a speed limit detection system would continue to consider valid the limitation ended by the de-restriction sign, and receiving wrong information would induce the driver to distrust the system.

To address this problem, a circular traffic sign detector based on shape detection could be a correct solution [6]. Anyway processing the whole image searching for circular shapes can be a difficult and expensive task, especially considering that the same system is already running the algorithm to detect the other signs. For these reasons, the proposed algorithm detects region of interest identifying patterns compatible with the other distinctive feature of the Italian de-restriction sign: the skewed black band. Then, since different elements generate pattern of this kind, the implemented algorithm searches around the candidate bands the circle corresponding to the edges of the sign. Additionally, the output is checked by means of tracking, which validates the sign when it is detected at least in two frames. The algorithm has been tested on 640×480 and 752×480 images taken with a $1/3$ inch sensor camera mounting a 6mm focal length lens.

Fig. 1. Examples of de-restriction signs treated by the algorithm.

The remainder of this paper is organized as follows. In Section II we present the black skewed band extractor. Section III describes the circle shape detector. The implemented tracking is illustrated in section IV. Section V provides some experimental results, while section VI is devoted to the discussion. Conclusions are drawn in Section VII.

## II. SKEWED BAND DETECTION

For each row of a grey-scale image, the band of a de-restriction sign causes a bright-dark-bright transition from the white background on the sign to the black band and back to the white background: in this case the distinctive feature of the band is not represented by its brightness, but by the couple of opposite grey level variations at its side borders. Coping with a similar problem, [7] presents a lane-markings extractor based on the fact that the width of the line to be detected is in a small range of values: for each row of the image, this range is determined in function of the expected width, that depends on the perspective in the image, and considering a little variability of the line marking width in the real world. The compatibility of the features found with a real line width is determined at this stage. Similarly, in our approach it is considered that the width of a de-restriction sign band can vary (it depends on the

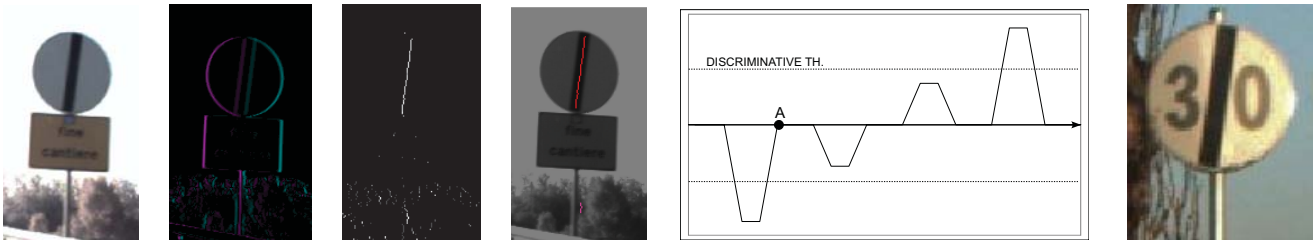


(*a*) (*b*) (*c*) (*d*) (*e*) (*f*)

Fig. 2. (*a*) De-restriction sign to be detected. (*b*) Derivative image: red and green highlight respectively negative and positive grey level variations. (*c*) LDL image: for better visualization the values, that represent the width of the band found, are normalized to the maximum possible value and multiplied by 255. (*d*) The labels found. (*e*) Graph of the values in a section of a row of the derivative image. (*f*) In this bent sign the left side is shaded and its brightness differs from that of the right side: with a restrictive threshold the LDL pattern would not be validated.

distance of the sign from the camera), but, unlikely [7], the width can be considered correct only after consideration about the ratio with the vertical length of the band it belongs to. For this reason, the proposed algorithm highlights, for each row of the image, center of regions between a negative and a positive variation in the image rows, creating a Light-Dark-Light (LDL) image that contains information about the width of the features found. Vertical chains of continuous and coherent pixels in the LDL image are then examined in order to select elements compatible with a black band of a de-restriction sign.

### *A. Light-Dark-Light pattern search*

To point out the grey level intensity variations, the algorithm applies a simple derivative filter with form (-1 0 1) on the image, obtaining a derivative image (fig. 2b).

For each row occupied by the de-restriction sign, the black band generates in the derivative image a specific pattern formed by:

- a negative peak, caused by the light-dark transition from the background on the sign to the band;
- a set of close-to-zero values, generated by the nearly constant value pixels within the band; the width of this region depends on the distance of the sign from the camera (and on the camera setup);
- a positive peak, caused by the dark-light transition from the band to the background on the sign.

To detect this pattern the algorithm scans from left to right the rows of the derivative image, obeying the rules explained in the following.

When a pixel with a negative value is found, a threshold is created (**discriminative threshold**) to discriminate among **negative**, **close-to-zero** and **positive** values. The discriminative threshold is set in proportion to the peak (absolute) value in a right neighborhood of the pixel.

The **state diagram** in figure 3 is then followed:

- After having received the first negative value and created the discriminative threshold, the system passes from state 0 to state 1, where the width of the negative peak is measured.
- When the first close-to-zero value is received, the system passes from state 1 to state 2, where the width of the nearly constant area is measured (i.e. the supposed width, expressed in pixel, of the band).
- Then, when a positive value is received, the system passes from state 2 to state 3, where the width of the positive peak is measured;
- Finally, when a non-positive value causes the system to exit from state 3, the pattern is validated if:
  - the transitions into and out from the band are quick enough (namely, if the width of the negative and the positive peak are under a certain threshold);
  - in the original image the brightness of the region on the left of the band and the brightness of the region on the right of the band are similar. We found that the threshold used to determinate this similarity cannot be set too restrictive because both of particular lighting conditions (see figure 2f) and of drawings that may be present to specify the ended prescription.
- A validated pattern is coded in a new image, named Light-Dark-Light (LDL) image, turning on a single pixel at the same coordinates of the center of the sequence found, giving it a value corresponding to the width of the close-to-zero sequence. In this way, in the LDL image the band becomes a segment with nearly constant value (see figure 2c).
- If the sequence from state 0 to state 3 is not correctly followed, the system drops to state 0 or 1 as shown in the diagram.

A shady sign placed on a light background (figure 2a) generates a particular graph of the values in the rows of the derivative image as shown in figure 2e: the highest negative and positive peaks are caused by the transition from the light sky in the background to the sign and then back to the background. On the other hand, the band of the de-restriction sign causes two smaller peaks, in the middle of the higher ones. When the highest negative peak is processed, it generates a discriminative threshold higher than the smaller peaks, so that they are considered close-to zero. In this way the pattern generated by the band would be discarded. To avoid this, when the system is in state 2, if the number of counted close-to-zero values exceeds a threshold the system

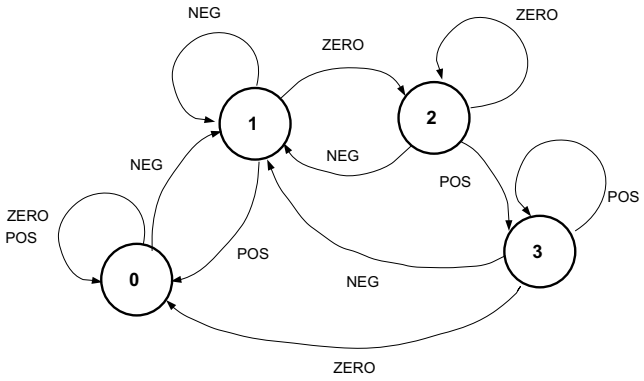


Fig. 3. LDL state diagram.

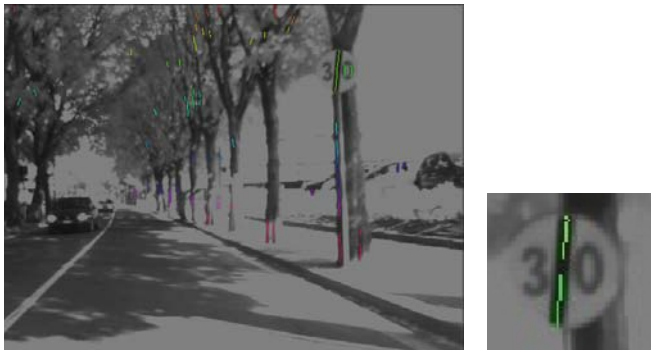

(*a*) (*b*)

Fig. 4. (*a*) Example of labeling results. (*b*) A broken label.

drops in state 0 and the processing restarts from the pixel on the right of the last negative peak detected (point A in the graph). The drawback of this choice is that the band can not be detected if it appears too wide in the image, i.e. if the sign is too close. With the configuration used for testing, the system proved to be able to detect the band when the sign was further than about 4 meters.

### *B. Labeling*

A de-restriction sign band is described by a vertical continuous area with constant width. In the LDL image this feature is coded as a vertical segment with nearly constant value, that is detected through the labeling process as explained in the following.

The width of the band of the de-restriction sign depends on its distance from the camera; since the detection is unreliable from excessive distances, a pixel can be considered "seed" of a label only if it represents a width of the band corresponding to a sufficiently close de-restriction sign, i.e. if its value in the LDL image is above a fixed threshold. This limits the maximum detection distance to about 20 meters with the configuration used for testing. The label is expanded iteratively examining the three pixels below the last added to the label. Note that only one of these pixels can be on, since by construction two pixels on in the same row of the LDL image are divided by at least two pixels off (considering the diagram in figure 3).

While expanding a label, statistics regarding the values of the labeled LDL image pixels are collected; to avoid detection and validation of black stripes with non-constant width, a new pixel is added to a label only if its value is close to the most frequent value among the pixels already included in the label.

The threshold used to find the seed pixel of the label is not applied during expansion, so that a band can be detected even if it is only partially of the required width. However, the seed pixel may be found not at the top of the band: since the expansion of the label is only downwards, the resulting label may miss its uppermost part. For this reason, after completing the labeling downwards, the seed of the label is expanded also upwards, following the same rules and using the statistics already collected. Finally, to cut off elements that are too short, the algorithm verifies that a label has a size greater than an adequate threshold. Figure 2d and figure 4a show two examples of labeling results.

### *C. Validation and union of label*

As figure 4a shows, at this point all elements that describe a black band (such as tree trunks and branches, windows, telephone cords, poles, etc) are labeled as candidate to be de-restriction sign bands. Moreover, elements drawn inside the de-restriction sign may act as noise sources at this stage, causing a partial miss-recognition of the Light-Dark-Light pattern previously presented; this failure entails the detection of a label split in two parts (fig. 4b).

To address these problems, the algorithm starts discarding elements that are too long, i.e. labels whose $\frac{length}{width}$ ratio is too high; then labels with a $\frac{length}{width}$ ratio in a restrictive range near the ideal one (estimated to be 8) are immediately selected for next step (sect. III).

To solve the problem concerning the detection of broken labels, still unselected labels are examined to check if they can be joined in order to generate a label with an adequate $\frac{length}{width}$ ratio. When the upper bound of a label is near to the lower bound of another label, the algorithm calculates the distance, on x-axis, between the upwards prolongation of the upper bound of the bottom label and the lower bound of the top label; if this result is lower than a threshold then the labels are joined. If the obtained label has a $\frac{length}{width}$ ratio compatible with the ideal one, it is selected for the next step.

Since the band of an Italian de-restriction sign is skewed, before proceeding the algorithm checks that the geometrical inclination of the selected labels is close to the ideal value (estimated to be -0.12 radians).

## III. CIRCLE DETECTION

In the next step, the algorithm verifies the presence of a circle, caused by the edge of the sign, around the selected labels. In the case studied we do not need to know the circle position nor its size, but just its presence, and the following

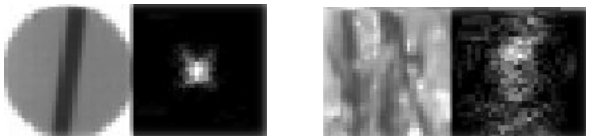

Fig. 5. Circle Hough Transform (CHT) in presence and in absence of a circle. To better comprehension the results are drawn normalizing the values to the highest one and multiplying them by 255.

(*a*) (*b*) (*c*)

Fig. 6. (*a*) Sign with only partially visible edges. (*b-c*) Example of mask applied during CHT computation. The mask limits wrong contributes caused by the band and by the drawn indication.

simplifications (**properties**) have been applied for the search of circles:

1) We already know where the circle should be, so that the search region is limited.
2) The circle center is expected to be in the middle of the band found.
3) We have an estimation of the expected circle diameter, given by the length of the band found.

Exploiting property 1, the algorithm identifies a bounding box around each detected band, i.e. a square region that is supposed to contain a circle; each bounding box is cropped from the input image and rescaled in order to obtain a 30×30 image, used to compute a Circle Hough Transform (**CHT**, see figure 5). The presence of a circle produces a concentration of high values in the central area of the bounding box; on the other hand, if the bounding box does not contain a circle, this concentration is missing.

Many circle detectors based on different kinds of CHT are proposed in literature. [8] presents an approach based on the radial symmetry, a variant of the CHT that looks for pairs of symmetrically oriented edges. Each pair defines completely a possible circle, and votes for the coherent center position and radius. This algorithm is fast (13.2 ms per 240×320 image frame on P3@1.4GHz) and gives high quality results. Anyway, this method would face difficulties in case of circle edges partially missing, e.g. caused by image saturation (fig. 6a). Exploiting the mentioned simplifications of the case studied, we decided to extend the sensitivity of our circle detector to address also this situations.

The implemented circle detector is based on a very well known method [9] that uses Sobel edge phase to reduce to two the dimension of the Circle Hough Transform. Figure 7 shows a graphical explanation.

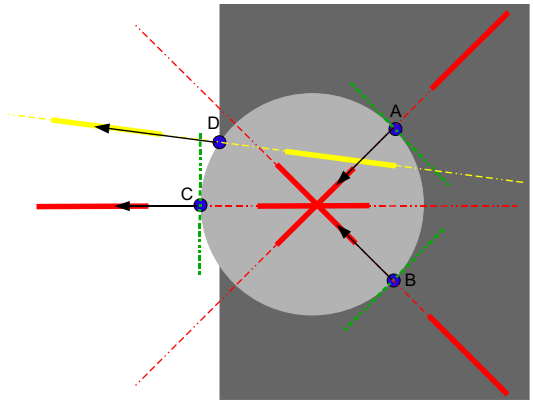


Fig. 7. Implemented voting system for CHT: every edge point votes along a line (dashed red) whose direction is that of the gradient of the image (black arrow), computed through a Sobel edge detector. Only two sections of the line are considered, namely those constituted by the points at a distance from the edge point in the interval $(r_{min}, r_{max})$ (solid red segments). $r_{min}$ and $r_{max}$ are chosen in a neighborhood of the expected radius, which is obtained following property 3. The segments are drawn in a new image of the same size using a rastering function inspired from the well known Bresenham Algorithm [10]. Points A, B and C contribute with one segment each passing through the center, causing a concentration of votes. The noise from the background causes a rotation of the Sobel phase for edge point D, whose votes (solid yellow) will not contribute to the correct detection of the circles.

Only Sobel edges vote, so that the choice of the threshold to be used becomes critical. [9] presents the tuning problem of Sobel and CHT thresholds: it is very difficult to find a set of parameters that allows the detection of all circles (even ones with low contrast) without getting false positives. In our case, being the region of interest very limited, the Sobel threshold can be kept very low, allowing most of the pixels to vote and keeping a good $\frac{signal}{noise}$ ratio, increasing the number of cases where the sign can be detected (see figure 8).

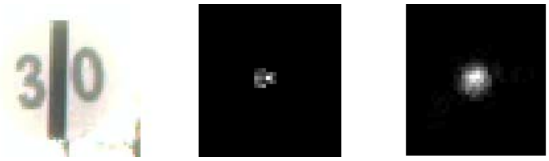

(*a*) (*b*) (*c*)

Fig. 8. (*a*) Sign in light contrast with the background. (*b*) Using a high Sobel threshold, in the CHT there are not enough contribution to determine the center of the circle, while (*c*) using a permissive threshold a high quality CHT is obtained, despite the initial low contrast.

The possibility to keep a low Sobel threshold would not be available if the CHT had to be computed on the whole image because many contributes would show up: along with the computational reasons, this is the main motivation why the implemented algorithm performs the band detection to highlight region of interest followed by the circle detection rather than vice versa.

In [8] the authors also dealt with the problem about the noise during the evaluation of the edge phase; with the drawing in figure 7 we want to emphasize a particular but

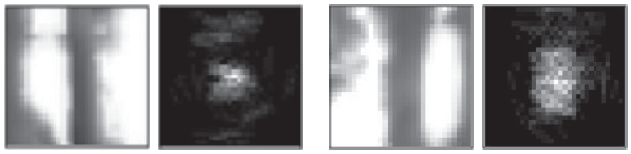

(*a*) (*b*) (*c*) (*d*)

Fig. 9. Examples of challenging patterns. (*a, c*) Tree trunks can generate black stripes compatible with a band of a de-restriction sign, while branches can form circle-like shapes. Anyway, both patterns are discarded because in the CHT (*c*) the center area collects too few votes or (*d*) the concentration of votes is not sufficiently compact.

significant case of this problem: because of an edge in the background, point D has a higher gradient norm with respect to the other circle border points; however, the edge in the background causes also a rotation of the gradient, so that point D gives a noise contribution (drawn in yellow) during circle detection. It can then be stated that favoring pixels with higher gradient during the voting process may lead to worse results.

In order to increase the $\frac{signal}{noise}$ ratio, a mask is defined to exclude all contributes brought by pixels of the input image expected to belong to the band or to the central zone of the sign, where a drawing may be present (fig. 6b, 6c).

A concentration of votes around the center of the CHT implies the presence of the expected circle. To identify this, a center area is defined (exploiting property 2) and two checks are performed:

- The mean value of the pixels in the center area must be over a threshold (enough positive votes are collected, see figure 9a, 9b)
- The ratio between the sum of the values in the center area and in the whole CHT must be over a threshold (concentration of the votes, see figure 9c, 9d)

Many challenging patterns are discarded during this step, like the crossing sign in figure 10. Anyway, sometimes properties 2 and 3 are not verified, causing a miss-detection. Figure 11 shows an example where the band of the sign is partially hidden. The detected label is not complete, so that the circle center and radius are wrongly estimated. This problem would be solved increasing the size of the region of interest around the band, and performing circle detection with less restrictive radius hypothesis and allowing the center of the circle to be possibly also not at the center of the CHT.

Input image Bounding box Hough Image

Fig. 10. Example of correct invalidation through CHT.

The performed process causes a small number of false positives. On the other side many factors (such as blurred frames) can cause intermittent detection.

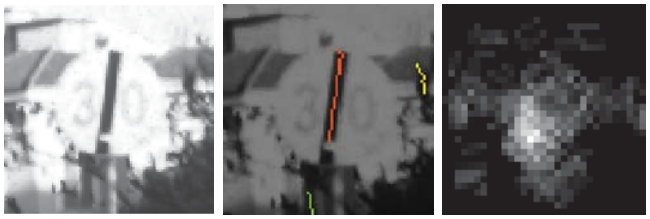

Input image Labeling Hough Image

Fig. 11. Partially hidden band. In the CHT, the concentration is not centered so that the circle is not detected.

## IV. TRACKING

To cope with intermittent detection and with the few false positives, the presented approach uses a simple tracking technique, that does not output the detected sign before its second detection and delete a previously detected sign after two missed detections. To decide if a previously detected sign is detected again, the algorithm checks if its bounding box, moved to an estimated position in the image for the current frame, overlaps with a sign detected at the current frame. If more than one sign is detected, old and new signs are coupled favoring best overlapping scores (OS):

$$OS_{ij} = \frac{A_{ij}}{max(A_i, A_j)} \quad i \in \{1 \dots N\},\ j \in \{1 \dots M\}$$

where $A_i$ is the area of the bounding box of the $i$-th sign detected at the previous frame, $A_j$ is the area of the bounding box of the $j$-th sign detected at the current frame, and $A_{ij}$ is their overlapping area. The position in the image of a previously detected sign at the current frame is estimated summing its speed to its last position. This speed is estimated as the movement (in $(x, y)$ image coordinates) of the center of the bounding box between two detections of the tracked sign over the number of frames (1 or 2) past between them. The example in figure 12 shows a sign tracked over 6 frames.

Although this simple tracking technique works correctly in most of the situations, image stabilization would help to improve results in case of road surface irregularities, that are likely to be present since a speed bumper may be placed between the restriction and the de-restriction sign. It would be also interesting to evaluate the results obtainable through a Kalman filtering, using a model that considers both the movement of the vehicle towards the sign and the terrain irregularities.

## V. RESULTS

Tested on more than 10,000 day light frames, the algorithm proved its robustness with 35 Italian de-restriction signs detected out of 37 and 2 false positives. A detection means that the sign is found for at least 2 consecutive frames (or separated by only 1 frame with missed detection). The two undetected signs are the one with the band partially hidden (fig. 11) and that shown in figure 13c, that does not have any contrast with the background so that the circle is not visible. If the number of detections necessary to send to the

Fig. 12. Example of tracking behavior in case of high driving speed ($\sim$ 90 Km/h, images taken with a 12 Hz frame rate). From top to bottom and from left to right: (*a*) The sign is recognized for the first time. (*b*) The sign is sent to the output when it is detected for the second time. The two detections overlap because the sign is still far and the movement in the image is small. However, at this point, it is possible to estimate the speed of the sign in the image (by the movement measured) and its expected position for the next frame: without this expedient it would not be possible to match the detected sign from (*c*) to (*d*) and from (*d*) to (*e*), where the movements are greater than the size of the bounding box. (*f*) The sign is too close to the camera (see section II) so that it is not detectable anymore. Anyway the position of the sign is estimated with good approximation; the bounding box is kept for one frame and sent to the output. The mismatch at next frame will cause the bounding box deletion.

output the sign is raised to 3, the statistics becomes 33 correct detection out of 37 signs with 0 false positives.

The detection succeeds with different kind of Italian de-restriction signs (figures 13a, 13b, 13g, 13h and 13j). The algorithm works correctly if there is contrast between the sign and the background (also in case of light contrast as shown in figure 13b), but if the edges of the sign are completely not visible, the detection fails (figure 13c).

Figures 13n and 13o exemplify the reliability of the algorithm in presence of many noise elements that generate patterns compatible with a de-restriction band. The detector is tolerant to rolled signs and to rolled input images, where the de-restriction band may not appear as skewed as expected (figure 13a, 13d); figure 13d also shows a case of successful detection in presence of a sign partially placed on a saturate background. Furthermore, the algorithm is robust to shadows and different illumination conditions (fig. 13e, 13f, 13k, 13l), and can overcome other cases of defective images, such as blurred images (fig. 13i).

Computation times were measured on a P4@2.8GHz system processing 640×480 images, examining the principal tasks of the algorithm separately:

- *LDL*: derivative image and LDL image computation;
- *Labeling*: labeling function and checks on labels;
- *CHT*: circle detection.

The first two tasks require constant times: 6ms for LDL and 2ms for Labeling. For CHT the computation time depends on the number of bounding boxes to be processed, but it is nearly constant for each circle detection (450$\mu$s) because of the resampling to 30×30 images. In a computationally expensive frame as that shown in figure 4a (9 regions of interest detected) the total computation time required by CHT is 4ms.

## VI. DISCUSSION

While danger and prescription signs were designed to be easily noticeable, de-restriction signs do not need immediate attention from the driver, so that no peculiar feature was assigned to them. In this way, their detection becomes very challenging because it is difficult to perform a search of regions of interest in the image. We decided to address this problem with a focused approach, that makes the designed algorithm very centered on this single task. Other more general approaches are proposed in literature for regions of interest detection, as white detection algorithms in [2], [11] and circle detection based. Anyway, none seems to be sufficiently independent of lighting and background conditions.

The algorithm has been tested on demanding images, in order to check for its robustness on different lighting conditions and even to defective images. To achieve an almost complete detection, thresholds were kept very low causing a few false positives to appear. Anyway, discarding the cases of dark, blurred or saturated images, thresholds can be increased removing these false positives. However, the test set should be extended, also including images taken by night.

In Europe, the most part of restrictions begun by a sign are not ended by a de-restriction sign: in fact, an intersection with another road ends the restriction if the restriction sign is not repeated after the intersection itself. It should be noticed that, for these reasons, signs like the ones indicating crossings and roundabouts define where a restriction is going to end. Anyway this problem does not seem to be easily addressable only with vision: even with a perfect intersection detector it would be almost impossible to distinguish between a real crossing and a private driveway access. Maps and GPS usage may help in locating intersections and in determining default speed limts based on vehicle location (e.g. in town, out town, or highway).

## VII. CONCLUSIONS

This paper describes an algorithm designed specifically to recognize Italian de-restriction signs, which are not easily detectable through a color based approach. The algorithm

Fig. 13. De-restriction sign detection (although the algorithm processes the whole image, only the right half of the image is showed for space reasons): (*a*) detection of two de-restriction signs in the same image; (*b*) with light contrast between the sign and the background; (*c*) without contrast between the sign and the background, the sign can not be detected; (*d*) in a rolled image, in presence of partially saturate background; (*e*) in a dark image; (*f*) spot shadows; (*g*)-(*h*) end of 50 and 70 km/h speed limit; (*i*) in a blurred image; (*j*) sign placed on the ground; (*k*) top and bottom of the sign differently enlightened; (*l*) right and left sides of the sign differently enlightened; (*m*) smaller, inside a square panel; (*n*) partially saturated background; (*n*)-(*o*) with trees; (*p*) false positive.


Fig. 14. Examples of Spanish (left) and German (right) de-restriction signs.

performed well in the tests carried out, with high percentage of detection and very few false positives. The computation is fast enough to be performed on the same machine where another color based traffic sign detector is running. The range of distances where the sign can be detected strictly depends on the acquisition system used (e.g. on the focal length); anyway a de-restriction sign does not need to be communicated to the driver in a particularly prompt way.

The investigation of this specific case has shown new opportunities that are going to guide future developments of our color based detector, e.g. introducing Sobel phase image analysis for better shape detection and region of interest cropping. Future developments of the de-restriction sign detector will regard removal of strong assumptions about radius length and center position during circle shape detection, application of neural networks to remove the remaining false positives and to recognize the specific limitation ended by the de-restriction sign, and extension of the algorithm to detect other countries de-restriction signs (fig. 14).

## ACKNOWLEDGMENT

The authors would like to thank Magneti Marelli Electronics Systems for the substantial support to this research.

## REFERENCES

[1] Alberto Broggi, Pietro Cerri, Paolo Medici, Pier Paolo Porta, and Guido Ghisio, "Real Time Road Signs Recognition," in *Procs. IEEE Intelligent Vehicles Symposium 2007*, Istanbul, Turkey, June 2007, pp. 981–986.

[2] Saturnino Maldonado Bascon, Sergio Lafuente Arroyo, Pedro Gil Jimenez, Hilario Gomez Moreno, and Francisco Lopez Ferreras, "Road-sign detection and recognition based on support vector machines," *ITS*, vol. 8, no. 2, pp. 264–278, June 2007.

[3] A. De La Escalera, J.M. Armingol, J.M. Pastor, and F.J. Rodriguez, "Visual sign information extraction and identification by deformable models for intelligent vehicles," *ITS*, vol. 5, no. 2, pp. 57–68, June 2004.

[4] Chiung-Yao Fang, Sei-Wang Chen, and Chiou-Shann Fuh, "Road-sign detection and tracking," *ITS*, vol. 52, no. 5, pp. 1329–1341, Sept. 2003.

[5] C. Bahlmann, Y. Zhu, Visvanathan Ramesh, M. Pellkofer, and T. Koehler, "A system for traffic sign detection, tracking, and recognition using color, shape, and motion information," in *Intelligent Vehicles Symposium (IV2005), Las Vegas, USA*, June 2005, pp. 255–260.

[6] N. Barnes and A. Zelinsky, "Real-time radial symmetry for speed sign detection," in *IEEE Intelligent Vehicle Symposium (IV2004), Parma, Italy*, June 2004, pp. 566–571.

[7] S.-S. Ieng, J.-P. Tarel, and R. Labayrade, "On the design of a single lane-markings detector regardless the on-board camera's position," in *IEEE Intelligent Vehicle Symposium (IV'2003)*, Columbus, OH, USA, 2003, pp. 564–569, http://perso.lcpc.fr/tarel.jean-philippe/iv03.html.

[8] Gareth Loy and Alexander Zelinsky, "Fast radial symmetry for detecting points of interest," *IEEE Trans. Pattern Anal. Mach. Intell.*, vol. 25, no. 8, pp. 959–973, Aug. 2003.

[9] Tilo Burghardt, "Circle detection in images using classic sobel filter and hough transformation," Tech. Rep. COMS 30121, University of Bristol, 2003.

[10] Jack Bresenham, "Algorithm for computer control of a digital plotter," *IBM Systems Journal*, vol. 4, no. 1, pp. 25–30, 1965.

[11] Jose M. Armingol, Arturo de la Escalera, Cristina Hilario, Juan M. Collado, Juan Pablo Carrasco, Marco Javier Flores, Jose Manuel Pastor, and F. Jose Rodriguez, "Ivvi: Intelligent vehicle based on visual information," *Robotics and Autonomous Systems*, vol. 55, no. 12, pp. 904–916, 2007.